

Luminescence and absorption in short period superlattices

M.F. PEREIRA*

*Department of Condensed Matter Physics, Institute of Physics CAS
Na Slovance 1999/2, 182 21 Prague 8, Czech Republic*

**email: pereira@fzu.cz*

Abstract - This paper applies analytical approximations for the luminescence of short period semiconductor superlattices and analyses the low density regime, demonstrating that the theory clearly connects with low density absorption with ratios of oscillator strengths of bound and continuum states as expected from the Elliott formula. A numerical study illustrates in detail the bleaching of higher order bound state. The analytical expressions have potential for systematic studies of controlled excitonic pathways characterized by THz responses.

Keywords: semiconductors superlattices, excitons, many body effects, absorption, luminescence, Terahertz, TERA-MIR

1 Introduction

A full understanding of how photoexcitations evolve into Coulomb-bound electron and hole pairs, called excitons, and unbound charge carriers is a key cross-cutting issue in photovoltaics and optoelectronics. Furthermore, these excitonic pathways are characterized by THz responses [1]. Consequently, systems where these effects can be controlled per design have strong potential for applications. Furthermore, semiconductor materials are the required substrate for Photoconductive Antennas, for which novel efficient solutions are constantly being sought [2] and semiconductor superlattices may become a successful and efficient substrate.

Semiconductor superlattices (SSLs) are media where the effective dimensionality of the electrons and holes can be controlled between two and three dimensions and are thus very important media to investigate transport and optical effects [3,4] from the GHz to the THz-Mid Infrared (TERA-MIR) range [5,6]. The smooth evolution from strongly localized quasi-two dimensional to highly delocalized quasi-three dimensional, notably for the relatively less studied inter-valence band case, may lead to interesting consequences for the coupling with light in nano and microcavities leading to polaritons [7].

The interest on semiconductor superlattices (SSLs) has been renewed due to the possibility of Terahertz (THz) radiation generation per frequency multiplication [8-14] and as model systems for nonlinear dynamics and band transport [15]. If SSL multipliers can be directly integrated with Gunn or Superlattice Electron Devices [16,17], the combination may become an alternative to quantum cascade lasers [18] in the low end of the THz spectrum. For a thorough, recent review and a comparison between electronic and optical sources of THz radiation, see Ref. [19].

It is thus timely to exploit different approaches for the theoretical description of optical properties of SSLs, such as luminescence, which is a very important tool to characterize new materials. As a matter of fact, recent research has led to analytical solutions of the Dyson equation for the polarization function, which is the self-energy in the Photon Green's function. Notably, the "s-shape" in the luminescence profiles as a function of temperature for these

materials have been studied in ternary GaAs_{1-x}Bi_x [20] and InAs_{1-x}N_x [21] as well as for more complex quaternary materials, such as InAs_{1-x-y}N_xSb_y [22], all in very good agreement with experimental data from different teams [23-26]. In a parallel effort, analytical solutions have shown that absorption nonlinearities increase with the anisotropy in SSLs [27-29].

This paper bridges the gap between these two lines of study and shows luminescence as a function of temperature and increasing anisotropy for short period SSLs with corresponding absorption, shows the connection between the equations and demonstrates that the approach reproduces the Elliott formula for excitons with the correct balance between bound and continuum states in the low density limit.

2 Mathematical Formalism

Nonequilibrium Green's Functions (NEGF) techniques including the photon Greens' function lead directly to expressions for the luminescence power spectrum and have reproduced both single beam and pump-probe luminescence experiments accurately [30-32]. They also lead to generalized semiconductor Bloch equations, can be applied to both intersubband [33-35] and interband transitions [36], but in both cases, require intensive numerical methods. The usual scattering mechanisms that affect the carriers transport are described by selfenergies [33] which lead to the absorption and luminescence linewidth. However, as highlighted in the introduction, analytical solutions based on controlled approximations have been recently developed. It is beyond the scope of this paper to repeat extensive derivations delivered in the references cited above. The important information to highlight is that the free photon Green's function represents the photons propagating without any interaction with the medium. When carriers are injected the transverse polarization function P , which is the selfenergy in photon Green's function Dyson equation, determines how the excited medium modifies the photon propagation. The lesser Keldysh component $P^<$ is proportional to the carriers recombination rate and yields the number of emitted photons per unit area. It thus governs the power emission spectrum through the relation

$$I(\omega) = (\hbar\omega^2/4\pi^2c) iP^<(\omega). \quad (1)$$

The imaginary and real parts of P^r are, respectively proportional to absorption/gain and refractive index changes, through the connection with the dielectric function of the medium

$$\epsilon(\omega) = 1 - \frac{c^2}{\omega^2} P^r(\omega). \quad (2)$$

For details, see Refs. [30-32]. Considering that for the excitation conditions of relevance for this paper, the (real) background dielectric constant $\epsilon(\infty) = n_b^2$, is much larger than both real and imaginary parts of the changes induced by the carriers, the absorption coefficient is thus

$$\alpha(\omega) = \frac{c}{2\omega\sqrt{\epsilon(\infty)}} \text{Im}\{P^r(\omega)\}. \quad (3)$$

The next step is to combine the Kubo-Martin-Schwinger (KMS) relation under the form derived in Ref. [29]

$$P^<(\omega) = \frac{-2i\text{Im}\{P^r(\omega)\}}{1 - \exp[(\hbar\omega - \mu)/(k_B T)]} \quad (4)$$

can be combined with Eqs. (1), (3) and the solution for the power spectrum [20, 37].

$$I(\omega) = \frac{I_0}{1 + \exp(\beta(\hbar\omega - \mu))} \left\{ \sum_{n=1}^{\sqrt{g}} \frac{4\pi}{n} \left(\frac{1}{n^2} - \frac{n^2}{g^2} \right) \delta_{\Gamma}(\xi - e_n) + 2\pi \int_0^{\infty} \frac{\sinh(\pi g \sqrt{x})}{\cosh(\pi g \sqrt{x}) - \cos(\sqrt{4g - g^2 x})} \delta_{\Gamma}(\xi - x) dx \right\}, \quad (5)$$

to deliver the direct connection with the absorption spectrum

$$\alpha(\omega) = \alpha_0 \vartheta \left\{ \sum_{n=1}^{\infty} \frac{\text{Int}\{\sqrt{g}\}}{n} \frac{4\pi}{n} \left(\frac{1}{n^2} - \frac{n^2}{g^2} \right) \delta_{\Gamma}(\zeta - e_n) + \int_0^{\infty} \frac{2\pi \sinh(\pi g \sqrt{x})}{\cosh(\pi g \sqrt{x}) - \cos(\pi \sqrt{4g - g^2 x})} \delta_{\Gamma}(\zeta - x) dx \right\}, \quad (6)$$

where $I_0 = \frac{\hbar \omega^2 e^2 |\langle S|x|X \rangle|^2 (E_g^0/\hbar)^2}{\pi e_0 c^3 a_0^3}$, $e_n = -\frac{1}{n^2} \left(1 - \frac{n^2}{g}\right)^2$, $n = 1, 2, 3, \dots$, $\zeta = (\hbar \omega - E_g)/e_0$, $g = (\kappa a_0)^{-1}$ where κ is the inverse screening length, and a_0, e_0 denote, respectively the exciton Bohr radius and binding energy, $\vartheta = \tanh[\beta(\hbar \omega - \mu)/2]$ and

$$\alpha_0 = \left(\frac{e^2}{\hbar c}\right) \left(\frac{E_g^0}{\hbar \omega}\right)^2 \left(\frac{\hbar \omega}{e_0}\right) \left(\frac{d^2}{a_0^3}\right) \frac{1}{\sqrt{\epsilon(\infty)}}. \quad (7)$$

The first term in the RHS of Eq. (7) is the dimensionless fine structure constant and $e^2 d^2 = e^2 |\langle S|x|X \rangle|^2$ is the dipole moment between the conduction and valence bands at $k = 0$. Note that in the spectral region around the bandgap where excitonic corrections are stronger, $\hbar \omega \sim E_g^0$ and the second term on the RHS of Eq. (7) can be

approximated by $\left(\frac{E_g^0}{\hbar \omega}\right)^2 \sim 1$ and consequently, $\alpha_0 \sim \left(\frac{e^2}{\hbar c}\right) \left(\frac{\hbar \omega}{e_0}\right) \left(\frac{d^2}{a_0^3}\right) \frac{1}{\sqrt{\epsilon(\infty)}}$.

The approximation used for renormalized bandgap is [36]

$$E_g = E_g^0 + e_0 \begin{cases} -1 + \left(1 - \frac{1}{g}\right)^2, & g \geq 1 \\ -1/g, & g < 1 \end{cases} \quad (8)$$

In the low density excitonic limit, $g \rightarrow \infty$, $\vartheta \rightarrow 1$, $e_n \rightarrow -\frac{1}{n^2}$, $E_g \rightarrow E_g^0$, leading to the Elliott formula [37]

$$\alpha(\omega) = \alpha_0 \left\{ \sum_{n=1}^{\infty} \frac{4\pi}{n^3} \delta_{\Gamma}(\zeta - e_n) + \int_0^{\infty} \frac{\pi e^{\pi/\sqrt{x}}}{\sinh \pi/\sqrt{x}} \delta_{\Gamma}(\zeta - x) dx \right\}, \quad (9)$$

showing that both luminescence and absorption formulas have the correct balance between bound and continuum states.

3 Numerical Results

The numerical examples in this section are for short period superlattices with strong delocalization of the electron and hole wavefunctions can be described in many cases by anisotropic 3D media, characterized by in-plane and transverse (along the growth direction) effective masses and dielectric constants. The anisotropy parameter γ is given by the ratio between the in-plane μ_{\parallel} and perpendicular μ_{\perp} reduced effective masses, $\gamma = \mu_{\parallel}/\mu_{\perp}$, which are calculated from the non-interacting superlattice Hamiltonian \mathcal{H}_0 , for electrons and holes, i.e. $i = e$ or h ,

$$\frac{1}{\mu_{\parallel}} = \frac{1}{m_{e\parallel}} + \frac{1}{m_{h\parallel}}, \quad \frac{1}{\mu_{\perp}} = \frac{1}{m_{e\perp}} + \frac{1}{m_{h\perp}}, \quad (10)$$

$$\frac{1}{m_{i\parallel}} = \hbar^{-2} \partial^2 / \partial k_{i\parallel}^2 \langle \Psi | \mathcal{H}_0 | \Psi \rangle, \quad \frac{1}{m_{i\perp}} = \hbar^{-2} \partial^2 / \partial k_{i\perp}^2 \langle \Psi | \mathcal{H}_0 | \Psi \rangle$$

These can be calculated from the corresponding free carrier Hamiltonian, and full details of technique which delivered good agreement with experimental excitonic data, can be found in Ref. [4].

Figure 1 shows calculated absorption and corresponding luminescence using the parameters determined by anisotropic medium theory for a short period GaAs-Al_{0.3}Ga_{0.7}As superlattice with repeated barrier and well widths equal to 1.5 nm. The resulting effective masses are $m_{e\parallel} \approx 0.078$; $m_{h\parallel} \approx 0.126$, $m_{e\perp} \approx 0.082$ and $m_{h\perp} \approx 0.447$. These lead the anisotropy parameter $\gamma = 0.698$. The resulting exciton binding energy and Bohr radius are given respectively by $e_0 = 5.22$ meV and $a_0 = 11.3$ nm.

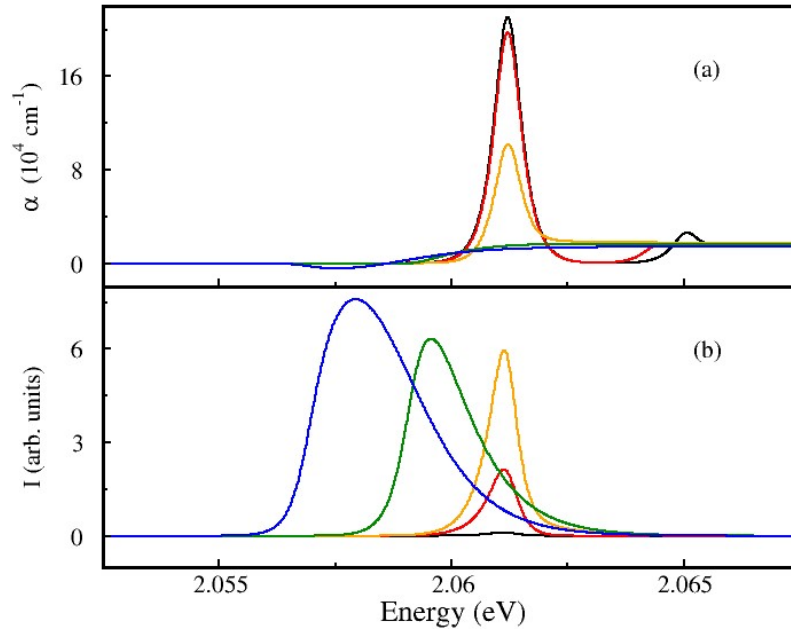


Fig.1 Absorption and luminescence of a short period GaAs-Al_{0.3}Ga_{0.7}As superlattice with repeated barrier and well widths equal to 1.5 nm. All curves have been calculated with the same broadening $\Gamma = 6.7$ meV and temperature $T=10$ K. The absorption $\alpha(\omega)$ of Eq. (6) is given in (a) from top to bottom (colour online) black, red, orange, green and blue correspond to carrier densities $N=1 \times 10^{13}$, 1×10^{14} , 1×10^{15} , 5×10^{15} and 1×10^{16} carriers/cm³. The luminescence $I(\omega)$ of Eq. (5) is given in (b) using the same colour convention to compare with the corresponding curves in (a).

The correct ratio of oscillator strength between bound and continuum states, highlighted by the exact limiting case in Eq. (9) is clearly seen. Both 1s and 2s states are visible at low density until they bleach out due to many body effects in absorption (Fig1.a), but it is difficult to see them in luminescence. The next figures highlight the effect in more detail.

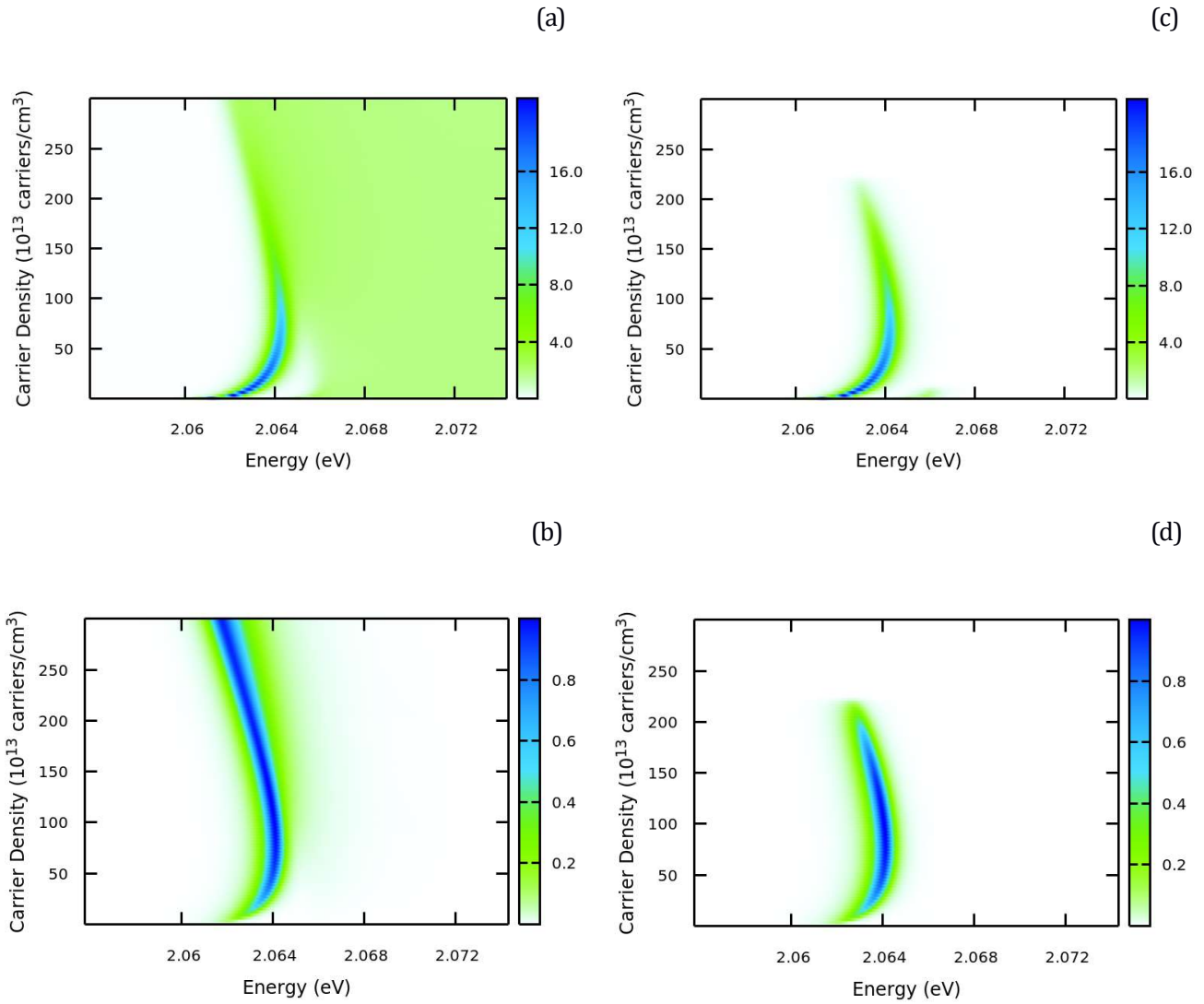
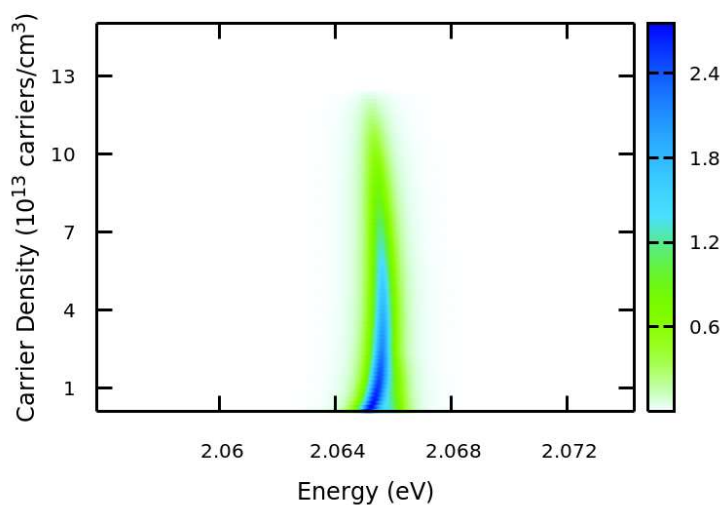


Fig.2 Absorption $\alpha(\omega)$ from Eq. (6) (a) and (b), compared with the corresponding luminescence from Eq. (5) for the same short period GaAs-Al_{0.3}Ga_{0.7} As superlattice of Fig. 1 and the same broadening $\Gamma = 6.7$ meV and temperature $T=10$ K. The full spectrum is shown in (a) and (b) while (c) and (d) have only the bound states contributions. The surface plots for absorption are given in $10^4 / \text{cm}^{-1}$ units exactly as in Fig. 1.a and the luminescence is in arbitrary units with the maximum scaled to 1.

Note the effect of the continuum in the absorption full green area in Fig.2.a. and the luminescence at high densities in Fig.2.b. Figures 1.c and 1.d show the contribution of bound states only and they are of course bleached due to many body effects at high densities. Note also the small absorption contributions beyond the 1S state around 2.065 eV in Figures 1.a and 2.c. These do not appear on luminescence on the same scale as the 1S contribution, because luminescence always favours the lowest energy transitions.

Contributions due to absorption beyond the 1S state, are shown in the detail in Fig. 3. The 1S luminescence maximum of Fig. 2.d is approximately 3299 times larger than the maximum of the sum of all bound states luminescence beyond 1S in Fig. 3.b.

(a)



(b)

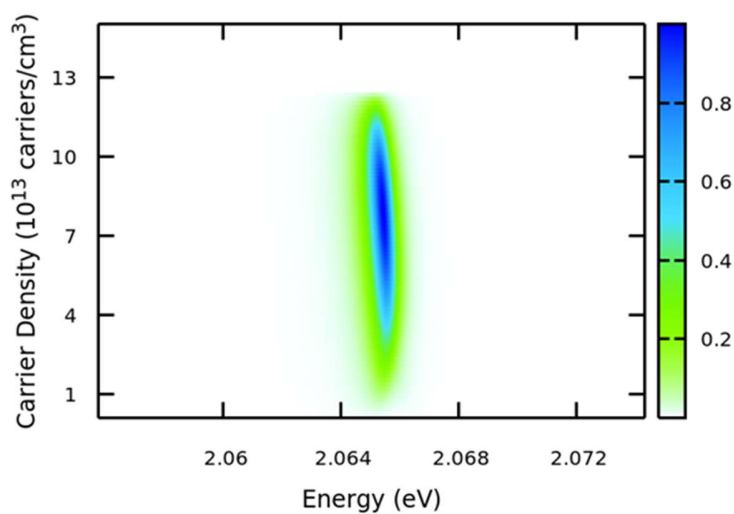


Fig.3 Absorption $\alpha(\omega)$ from Eq. (6) (a) and (b), compared with the corresponding luminescence from Eq. (5) for the same short period GaAs-Al_{0.3}Ga_{0.7} superlattice of Fig. 1 and the same broadening $\Gamma = 6.7$ meV and temperature $T=10$ K. Only the bound states contributions beyond the 1S are shown. The surface plot for absorption is given in 10^4 /cm⁻¹ units exactly as in Fig. 1.a and the luminescence is in arbitrary units with the maximum scaled to 1. The 1S luminescence maximum of Fig. 2.d is approximately 3299 times larger than the maximum of the sum of all bound states luminescence beyond 1S in Fig. 3.b.

Before summarizing the results obtained in this paper, two important points should be noted: an excellent review on many-body correlations and excitonic effects in semiconductor spectroscopy is given in Ref. [40], which has very useful relations and a connection to Elliott's formula, but to the best of our knowledge, the expressions introduced in Refs. [20, 37] and extended here, are the only fully explicit analytical solutions for the luminescence with Coulomb correlations which are directly programmable for bulk and superlattices in the anisotropic medium limit. Furthermore, effects such as the Urbach tail are only simulated by the choice of linewidth function δ_F . A predictive description is possible by including interactions with phonons and localized states by momentum independent selfenergies, such as those used in Ref. 10. Full frequency and momentum dependent selfenergies would prevent a direct use of the solutions of the Hulthén potential used in this paper.

In summary, this paper bridged the gap between luminescence and nonlinear absorption in short period superlattices, in which carrier tunnelling lead to quasi-three dimensional behaviour. The low density limit equations and the numerical results using the full formula demonstrate that the approach reproduces the Elliott formula for excitons with the correct balance. The bandgap renormalization used here is an approximation, but the important feature is to see the luminescence following consistently the evolution from absorption to gain with a simple analytical approach, in contrast to previous intensively numerical calculations. Details of high order bound states and their fast bleaching as a function of injected carrier densities are shown in detail. The accuracy and simplicity of the method should make it a powerful tool for research and development of new materials and devices and can play a role on a systematic control of excitonic pathways characterized by THz responses.

Acknowledgements: The author acknowledges support from the Programme "IMPA Verão 2018" of the Instituto de Matemática Pura e Aplicada (IMPA) in Rio de Janeiro, Brazil.

References

1. Luo, Liang; Men, Long; Liu, Zhaoyu; Mudryk, Yaroslav; Zhao, Xin; Yao, Yongxin; Park, Joong M.; Shinar, Ruth; Shinar, Joseph; Ho, Kai-Ming; Perakis, Ilias E.; Vela, Javier; Wang, Jigang, Ultrafast terahertz snapshots of excitonic Rydberg states and electronic coherence in an organometal halide perovskite, *Nature Communications* 8, 15565-1, 15565-8 (2017).
2. Lepeshov, S.I.; Gorodetsky, A.A.; Toropov, N.A.; Vartanyan, T.A.; Rafailov, E; Krasnok, A.E. and Belov, P.A, Optimization of Nanoantenna-Enhanced Terahertz Emission from Photoconductive Antennas, *Journal of Physics: Conference Series* 917, 062060-1 - 062060-4 (2017).
3. Wacker, A: Semiconductor superlattices: a model system for nonlinear transport, *Physics Reports* 357, 1-111 (2002).
4. Pereira Jr., M.F.: Analytical solutions for the optical absorption of superlattices, *Phys. Rev. B* 52, 1978-1983 (1995).
5. Pereira, M.F.: TERA-MIR radiation: materials, generation, detection and applications II, *Opt Quant Electron* 47, 491-493 (2014).
6. Pereira, M.F.: TERA-MIR radiation: materials, generation, detection and applications, *Opt Quant Electron* 47, 815-820 (2015)
7. Pereira, M.F. and Faragai, I.A.; Coupling of THz radiation with intervalence band transitions in microcavities, *Optics Express* 22, 3439-3446 (2014).
8. Gaifullin, M.B., Alexeeva, N.V., Hramov, A.E., Makarov, V.V., Maksimenko, V.A., Koronovskii, A.A., Greenaway, M.T., Fromhold, T.M., Patané, A., A. Mellor, C. J., F.V. Kusmartsev, F.V. and Balanov, A.G.:

Microwave Generation in Synchronized Semiconductor Superlattices, *Phys. Rev. Applied* 7, 044024 (2017).

9. Pereira, M.F., Winge, D., Wacker, A., Zubelli, J.P., Rodrigues, A.S., Anfertev, V. and Vaks, V.: Theory and Measurements of Harmonic Generation in Semiconductor Superlattices with Applications in the 100 GHz to 1 THz Range, *Phys. Rev. B* 96, 045306 (2017).
10. Pereira, M.F., Anfertev, V, Zubelli, J.P. and Vaks., V: THz Generation by GHz Multiplication in Superlattices, *J. of Nanophotonics*, 11(4), 046022-1 - 046022-6 (2017).
11. Alekseev, K.N., Erementchouk, M.V., and Kusmartsev, F.V.: Direct-current generation due to wave mixing in semiconductors, *Europhys. Lett.* 47, 595 (1999).
12. Alekseev, K.N., Cannon, E.H., Kusmartsev, F.V. and Campbell, D.K.: Fractional and unquantized dc voltage generation in THz-driven semiconductor superlattices, *Europhys. Lett.* 56, 842 (2001).
13. Alekseev, K.N. and Kusmartsev, F.: Pendulum Limit, Chaos and Phase-Locking in the Dynamics of Ac-Driven Semiconductor Superlattices, *Physics Letters A* 305, 281 (2002).
14. Alexeeva, N, Greenaway, M.T., Balanov, A.G., Makarovskiy, O, Patanè, A., Gaifullin, M.B., Kusmartsev, F. and Fromhold, T.M.: Controlling High-Frequency Collective Electron Dynamics via Single-Particle Complexity, *Phys. Rev. Lett.* 109, 024102 (2012).
15. Apostolakis, A., Awodele, M.K., Alekseev, K.N., Kusmartsev, F.V. and A. G. Balanov, A.G.: Nonlinear dynamics and band transport in a superlattice driven by a plane wave, *Phys. Rev. E* 95, 062203-1 - 062203-10 (2017).
16. Eisele, H., Khanna, S.P. and Linfield, E.H.: Superlattice electronic devices as high-performance oscillators between 60-220 GHz, *Appl. Phys. Lett.* 96, 072101 (2010).
17. Eisele, H.: 480GHz oscillator with an InP Gunn device, *Electron. Lett.* 46, 422 (2010).
18. Razeghi, M, Lu, Q.Y., Bandyopadhyay, N., Zhou, W., Heydari, D., Bai, Y., and Slivken, S.: Quantum cascade lasers: from tool to product, *Opt. Express* 23, 8462 (2015).
19. Razegui, M.: Recent progress of widely tunable, CW THz sources based QCLs at room temperature, *Recent progress of widely tunable, CW THz sources based QCLs at room temperature* 10, 87 -151 (2017).
20. Oriaku, C.I. and Pereira, M.F.: Analytical solutions for semiconductor luminescence including Coulomb correlations with applications to dilute bismides, *J. Opt. Soc. Am. B* 34, 321-328 (2017).
21. Oriaku, C.I., Spencer, T.J., Yang, X., Zubelli, J.P. and Pereira, M.F.: Analytical expressions for the luminescence of dilute quaternary InAs(N,Sb) semiconductors, *J. Nanophoton.* 11, 026005-1 - 026005-8 (2017).
22. Yang, X., Oriaku, C.I., Zubelli, J.P. and Pereira, M.F.: Automated Numerical Characterization of Dilute Semiconductors per Comparison with Luminescence, *Optical and Quantum Electronics* 49, 93-1 - 93-8, (2017).
23. Fluegel, B., Francoeur, S., Mascarenhas, A., Tixier, S., Young, E.C. and Tiedje, T.: Giant Spin-Orbit Bowing in GaAs_{1-x}Bi_x, *Phys. Rev. Lett.* 97, 067205 (2006).
24. Mazzucato, S., Lehec, H., Carrère, H., Makhoulfi, H.; Arnoult, A., Fontaine, C., Amand, T. and Marie, X.: Low-temperature photoluminescence study of exciton recombination in bulk GaAsBi, *Nanoscale Res Lett* 9, 19 (2014).
25. Latkowska, M. et al.: Temperature dependence of photoluminescence from InNAsSb layers: The role of localized and free carrier emission in determination of temperature dependence of energy gap, *Appl. Phys. Lett.* 102, 122109 (2013).
26. Krier, A., De la Mare, M., Carrington, P.J., Thompson, M., Zhuang, Q., Patanè, A., Kudrawiec, R.: Development of dilute nitride materials for mid-infrared diode lasers. *Semicond. Sci. Technol.* 27, 4009-1 - 4009-8 (2012).

27. Oriaku, C.I., Spencer, T.J. and Pereira, M.F.: Anisotropic Medium Approach for the Optical Nonlinearities of Dilute Nitride Superlattices, THz for CBRN and Explosives Detection and Diagnosis, Edited by M.F. Pereira and O. Shulika, pp.113-203, Springer (2017),
28. Pereira, M.F., Anisotropy and Nonlinearity in Superlattices II, *Optical and Quantum Electronics*, 48, 423-1 - 423 - 8 (2016).
29. Pereira, M.F., Anisotropy and Nonlinearity in Superlattices, *Optical and Quantum Electronics* 48, 321-1-321-7 (2016).
30. Pereira Jr., M.F. and Henneberger, K: Microscopic theory for the influence of Coulomb correlations in the light-emission properties of semiconductor quantum wells, *Phys. Rev. B*. 58, 2064 (1998).
31. Michler, P., Vehse, M., Gutowski, J., Behringer, M., Hommel, D., Pereira Jr., M.F. and Henneberger, K.: Influence of Coulomb Correlations on Gain and Stimulated Emission in (Zn,Cd)Se/Zn(S,Se)/(Zn,Mg)(S,Se) Quantum Well Lasers, *Phys. Rev. B*. 58, 2055 (1998)
32. Pereira Jr., M.F. and Henneberger, K.: Greens Functions Theory for Semiconductor Quantum Well Laser Spectra, *Phys. Rev. B*53, 16485 (1996).
33. Schmielau, T. and Pereira, M.F.: Momentum dependent scattering matrix elements in quantum cascade laser transport, *Microelectronics Journal* 40, 869-871 (2009).
34. Nelander, R., Wacker, A., Pereira Jr. M.F., Revin, D.G., Soulby, M.R., Wilson, L.R., Cockburn, J.W., Krysa, A.B., Roberts, J.S. Airey, R.J. :Fingerprints of spatial charge transfer in quantum cascade lasers, *Journal of Applied Physics* 102, 113104 (2007).
35. Pereira, M.F., :The Linewidth Enhancement Factor of Intersubband Lasers: From a Two-Level Limit to Gain without Inversion Conditions, *Applied Physics Letters* 109, 222102 (2016).
36. Pereira Jr., M.F., Binder, R. and S.W. Koch: Theory of nonlinear absorption in coupled band quantum wells with many-body effects, *Appl. Phys. Lett.* 64, 279 (1994).
37. Pereira. M.F: Analytical Expressions for Numerical Characterization of Semiconductors per Comparison with Luminescence, *Materials* 11, 2 (2018).
38. Banyai, L., and Koch, S.W.: A simple theory for the effects of plasma screening on the optical spectra of highly excited semiconductors, *Z. Phys. B*. 1986, 63, 283.
39. Haug. H and Koch, S.W.: *Quantum Theory of the Optical and Electronic Properties of Semiconductors*, (World Scientific, 2005).
40. Kira, M and Koch, S.W.: Many-body correlations and excitonic effects in semiconductor spectroscopy, *Progress in Quantum Electronics* 30, 155-296 (2006).